Size Selectivity of Narrow Pores

David Goulding, Jean-Pierre Hansen, and Simone Melchionna
Department of Chemistry, University of Cambridge, Lensfield Road, Cambridge CB2 3QZ United Kingdom
(Received 11 April 2000)

The selectivity of micropores and ion channels is examined for simple pore topologies within the framework of density functional theory of highly confined fluids. In an infinite cylindrical pore purely steric (excluded volume) effects are shown to lead to strong, nontrivial size selectivity, which is highly sensitive to the pore radius. A crude modeling of electrostatic effects does not alter the relative absorbance of Na^+ and K^+ ions in a significant way.

PACS numbers: 87.10.+e, 61.20.–p, 61.25.–f

The structural and transport properties of highly confined fluids differ considerably from their bulk behavior. This is, in particular, the case of liquids and solutions in microporous materials which are often found to act as filters with a high degree of molecular or ionic selectivity. Much studied examples include zeolites, where selectivity leads to specific catalytic activity [1], and ion channels through membranes, whose ion selectivity has considerable physiological implications [2]. The distribution and transport of ions and water molecules in narrow channels through a variety of membrane proteins have been the object of a number of recent Molecular Dynamics (MD) simulation studies, based on molecular models for water, ions and channel topology of various degrees of realism [3–8]. Such simulations provide valuable insight into mechanisms of ion selectivity and transport for specific ion channels, in particular the KcsA K^+ channel [7], the crystal structure of which has been recently determined by x-ray diffraction [9]. The selectivity and stabilization of ions within channels is expected to result from a subtle competition between steric (size) effects and electrostatics, which control the hydration and dehydration of the ions [4].

In this Letter we focus on generic packing aspects by considering a simple model to show that steric, excluded volume effects alone lead to an unexpectedly strong selectivity of particle size in cylindrical pores, which is of purely entropic origin. We consider the situation of an infinite cylindrical pore of radius R, with ends opening into infinite reservoirs containing a solution made up of three species: the majority component, or solvent, and two solutes. In the case of ion channels, the former would be water, and the latter would be the competing ionic species, say, Na^+ and K^+. In the present simplified model all three species are merely hard spheres (HS), of different diameters σ_α (see Fig. 1). No electrostatics is involved at this stage, but in explicit calculations bare ion and water diameters, $\sigma_{Na^+} = 0.194$ nm, $\sigma_{K^+} = 0.266$ nm and $\sigma_{H_2O} = 0.32$ nm were chosen throughout. In the bulk reservoirs, the reduced free energy per unit volume, $f = F/(Vk_BT)$, of the ternary HS mixture depends only on the diameters σ_α and packing fractions $\eta_\alpha = \pi n_\alpha \sigma_\alpha^3/6$ of the various species, where $n_\alpha = N_\alpha/V$ is the bulk number density of species α. f is known to a high degree of accuracy from the compressibility equation of state resulting from the analytic solution of Percus-Yevick (PY) theory for HS mixtures [10]; the chemical potentials μ_α of the three species follow directly from standard thermodynamic derivatives.

Within the cylindrical pore, on the other hand, the HS mixture becomes a highly inhomogeneous fluid dominated by surface effects, and characterized by position-dependent local densities $\rho_\alpha(\mathbf{r})$ of each species. In an infinite cylinder, confinement breaks translational invariance in the plane perpendicular to the cylinder axis (chosen as z axis), so that the density profiles vary rapidly, over molecular length scales, along any radial direction, and depend only on the distance $r = \sqrt{x^2 + y^2}$ from the axis. According to the basic principles of density functional theory (DFT) of nonuniform fluids [11], the density profiles may be determined by minimizing a free energy functional of the $\rho_\alpha(r)$, which generalizes the usual Helmholtz free energy function of the uniform densities n_α, valid in the bulk, to inhomogeneous situations. If $F[\{\rho_\alpha(r)\}]$ denotes this functional, and if the confined

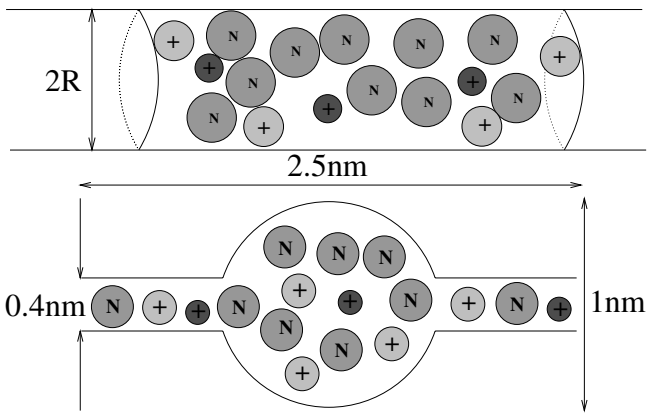

FIG. 1. Schematic representation of the two channel topologies considered in this paper. Model 1 is an infinite cylinder of radius R; model 2 is a finite pore with a spherical cavity R_0, flanked by two coaxial cylindrical segments on both sides. The circles give an idea of the relative sizes of Na^+, K^+ ions, and H_2O molecules used in this study.

 0031-9007/00/85(5)/1132(4)$15.00

fluid is in equilibrium with a bulk reservoir, which fixes the values of the chemical potentials μ_α of the various species, then the $\rho_\alpha(r)$ may be determined from the variational principle:

$$\frac{\delta F}{\delta \rho_\alpha(r)} = \mu_\alpha\,, \tag{1}$$

where the derivatives on the left correspond to functional differentiation.

The functional F is made up of three contributions, the ideal part $F_{\rm id}$ corresponding to noninteracting molecules, (i.e., an ideal gas), which is known exactly [11], an excess contribution $F_{\rm exc}$, arising from correlations between molecules, and a part describing the coupling to the external field of the confining surfaces, $F_{\rm ext}$. The nontrivial excess part is generally unknown and must be approximated in a way appropriate for a given physical situation. For multicomponent HS fluids, the most accurate and successful approximate functional $F_{\rm exc}$ is based on Rosenfeld's "fundamental measure" theory, which expresses the functional in terms of weighted (rather than bare) local densities [12], involving weight functions based on simple geometric considerations. Under the unconfined homogeneous conditions of the bulk, the Rosenfeld free energy leads back to the PY free energy derived from the compressibility equation of state; the latter allows the chemical potentials appearing on the right-hand side of Eq. (1) to be calculated, for a given composition of the reservoir.

The density profiles $\rho_\alpha(r)$ within the cylindrical pore are calculated by solving the three coupled Euler-Lagrange equations associated with the variational principle (1) for $\alpha = H_2O$, Na^+, and K^+. The contribution of the external field reduces here to the confinement constraints,

$$\rho_\alpha(r) = 0, \qquad r > R - \sigma_\alpha/2\,. \tag{2}$$

The purely radial Euler-Lagrange equations for the three profiles are easily solved numerically, subject to the constraints (2) and for given values of the μ_α. The latter were chosen to ensure equal concentrations of $1M$ of Na^+ and K^+ ions in the bulk, and a packing fraction of the HS solvent $\eta_{H_2O} = 0.41$. The resulting radial density profiles are shown in Fig. 2, for two cylinder radii, $R = 0.4$ and 0.5 nm, typical of ion channels. For $R = 0.4$ nm, the three profiles are dominated by layering near the channel surface. For $R = 0.5$ nm, the profiles exhibit a second peak near $r = 0$, signaling the appearance of an additional layer along the axis of the channel, as would be expected from simple packing considerations. These results are in overall qualitative agreement with the MD data of Lynden-Bell and Rasaiah [4] for a more realistic model of water, in the case where the charge of the ions is set to zero.

To assess the quantitative reliability of the functional used in the present calculations, which has not previously been tested under comparable conditions, we have carried out grand-canonical Monte Carlo (GCMC) simulations of HS mixtures confined to cylindrical pores, for physical parameters identical to those used in the DFT calculations. In GCMC simulations [13], in addition to the usual trial displacements of spheres, attempts are made to insert particles of the various species at random positions inside the cylinder, or to delete randomly chosen particles, according to a generalized Metropolis algorithm satisfying detailed balance, until chemical equilibrium is achieved with a reservoir of given chemical potentials. The present simulations involved cylinders of 20–30 nm length, with periodic boundary conditions along the z axis. Figure 2 shows that the DFT results compare very favorably with the "exact" simulation data, lending a high degree of confidence in the predictions of the computationally much less demanding DFT.

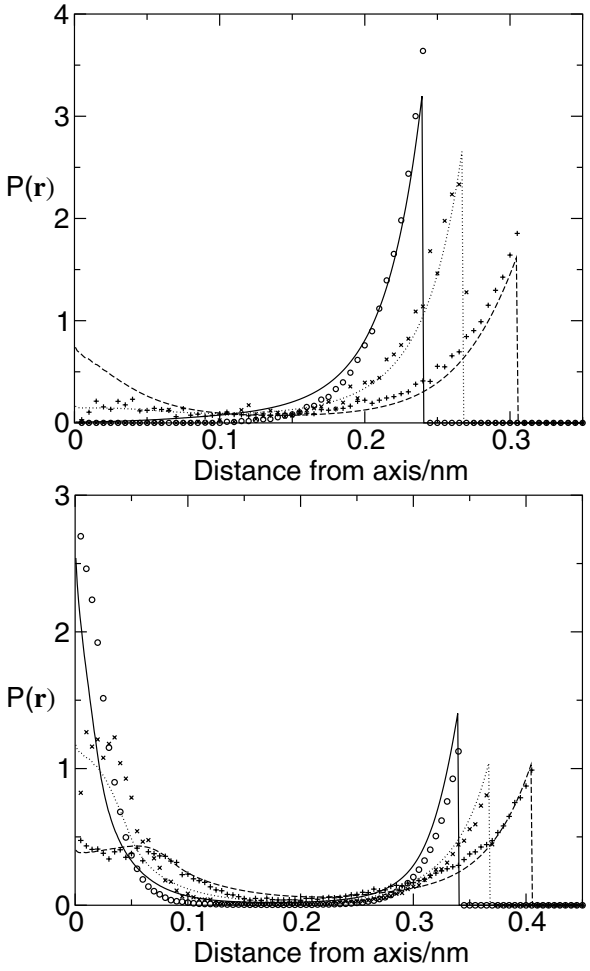

FIG. 2. Radial density profiles of Na, K ions and H_2O molecules in a cylindrical pore of radius $R = 0.4$ nm (upper curves) and $R = 0.5$ nm (lower curves). The ratios $\rho_\alpha(r)/n_\alpha$ are shown, where n_α is the bulk density in the reservoir, i.e., outside the channel. The DFT results are the dashed (Na), dotted (K), and solid (H_2O) curves, while the corresponding symbols for the Monte Carlo results are +, ×, and ∘. All data is for the hard sphere mixture model, where the Na^+ and K^+ are at a concentration of $1M$ in the reservoir.

The mean number of particles of species α per unit volume inside the channel is

$$\bar{\rho}_\alpha = \frac{2}{R^2}\int_0^R \rho_\alpha(r) r\, dr\,, \tag{3}$$

and we define the absorbance of species α to be the dimensionless ratio $\zeta_\alpha = \bar{\rho}_\alpha/n_\alpha$, where n_α is the bulk concentration of the species in the reservoir which, for the ions, is chosen to be close to the physiological concentrations, $0.05M$, in the following discussion. The absorbances of Na^+ and K^+ ions and of water molecules, as calculated from the HS mixture model, are plotted as functions of the channel radius R in Fig. 3. As expected, $\zeta_\alpha \to 1$ in the limit of large channels ($R \gg \sigma_\alpha$) and vanish for $R < \sigma_\alpha/2$. The absorbances of the two ionic species exhibit a considerable amount of structure up to $R \simeq 0.4$ nm. The competition of the two ionic species is illustrated in Fig. 4 which shows the relative absorbance $\zeta = \zeta_{Na^+}/\zeta_{K^+}$ as a function of channel radius R. For equal concentrations of the two species outside the channel (i.e., in the reservoir), the relative absorbance varies considerably with R, from a minimum value of about 0.2 for $R \simeq 0.16$ nm to a maximum value of almost 3 for $R \simeq 0.28$ nm. This rapid variation points to a very strong ion selectivity of cylindrical channels, due solely to steric effects. The unexpected result is that very narrow channels, of radius barely sufficient to let water molecules go through (i.e., $R \simeq 0.16$ nm), absorb the larger K^+ ion, while pores almost twice as large ($R \simeq 0.28$ nm) strongly favor the absorptions of the smaller Na^+ ion; increasing R further, to about 0.32 nm (corresponding to twice the radius of a water molecule), again favors K^+ absorption. The absorption of the minority ion species is relatively unaffected by their bulk concentrations inasmuch as the overall packing fraction is hardly changed by their presence.

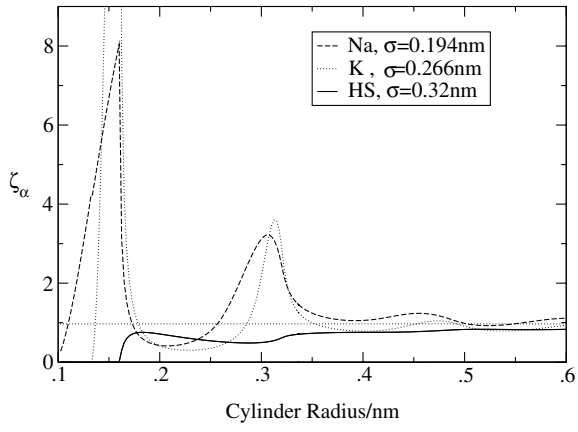

FIG. 3. Absorbances ζ_α of Na ions (dashed curve), K ions (dotted curve), and H_2O molecules (solid curve), as functions of the radius R of the cylindrical channel. The results are for the hard sphere mixture model. The K absorbance peaks at a value of about 30. The bulk concentrations for the K^+ and Na^+ are $0.05M$.

The relative absorbance ζ of Na^+ and K^+ can be reproduced by a simple free volume argument in the range $R < \sigma_{H_2O}$, i.e., for channels so narrow that the largest spheres cannot penetrate. In that limit the micropore contains only a small number of Na^+ and K^+ spheres, which behave essentially as a confined mixture of noninteracting particles, in chemical equilibrium with the highly correlated three-component mixture in the reservoir. The corresponding density profiles inside the cylinder are constant, subject to the constraints (2), and equal to

$$\rho_\alpha(r) = n_\alpha e^{\beta\mu_\alpha^{ex}}, \qquad r < R - \sigma_\alpha/2\,, \tag{4}$$

where $\beta = 1/K_BT$ and μ_α^{ex} is the excess (nonideal) part of the chemical potential of species α, set by the reservoir, where the bulk concentration is n_α. Substitution of (4) into (3) immediately leads to the following absorbance ratio for bulk equimolar solutes:

$$\zeta = \frac{(R - \sigma_{Na^+}/2)^2}{(R - \sigma_{K^+}/2)^2}\exp\{\beta(\mu_\alpha^{Na^+} - \mu_\alpha^{K^+})\}, \tag{5}$$

valid in the interval $\sigma_{K^+}/2 < R < \sigma_{H_2O}$. This result perfectly reproduces the rapid initial drop of ζ with R in Fig. 4.

The simple result (5) confirms, in particular, that the adsorbance of the smaller Na^+ ion is about 5 times less that of the bigger K^+ ion at $R = 0.16$ nm, i.e., just before the larger water spheres can enter the cylinder. The subsequent peak in the relative absorbance is confirmed by GCMC simulations carried out at the higher concentration of $1M$ for both species. The statistical uncertainties in these simulations increase greatly as the cylinder radius is reduced.

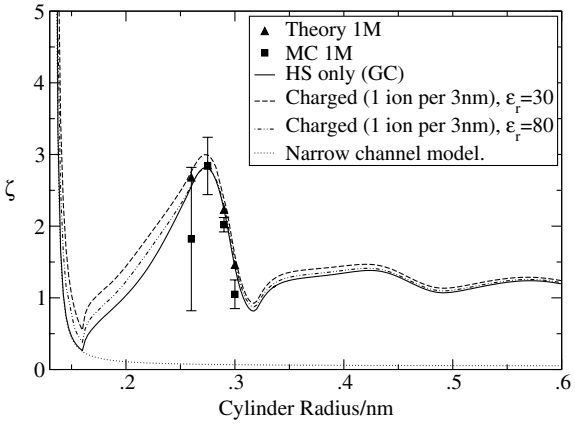

FIG. 4. Relative absorbance $\zeta = \zeta_{Na^+}/\zeta_{K^+}$ of Na^+ and K^+ ions in a cylindrical channel, as a function of cylindrical radius R. The solid curve is for the hard sphere mixture (corresponding to an infinite dielectric constant ϵ), while the dashed-dotted and dashed curves are for charged hard sphere Na^+ and K^+ ions, with $\epsilon = 80$ and 30. The lines are for bulk concentrations of K^+ and Na^+ of $0.05M$, while the squares are MC results with the associated error bars, and triangles are the corresponding DFT results for bulk concentrations of K^+ and Na^+ of $1M$. The dotted line is the fit to the model for very narrow channels described by Eq. (5).

The simple HS model thus predicts unexpectedly large variations of the relative size selectivity of cylindrical pores with their radius, due to entropic excluded volume effects alone. Clearly, the model is far too simplistic to do justice to the complexity of realistic micropores or ion channels. We have made preliminary investigations of two extensions of the present model.

In a first step towards a more complete description of ions in cylindrical pores we have endowed the ionic spheres with a central point charge, $+e$. The confining surface of the cylindrical channel is assumed to carry a uniform negative surface charge σ, such that the total system remains electrically neutral; σ was chosen such that the channel can accommodate, on average, one Na^+ or K^+ ion per 3 nm length. The water molecules are still assumed to be hard spheres, but the electrostatic interactions between charges are reduced by a factor $1/\epsilon$, where ϵ is the continuum dielectric constant of water. In other words, the excluded volume effects of water are treated on the molecular level, while the dielectric effects, linked to molecular multipoles and hydrogen bonding, are treated on a macroscopic continuum level. In bulk water at room temperature, $\epsilon \simeq 80$, but this value is known to be strongly reduced in highly confined geometries, due to the gradual breakup of the hydrogen-bond network and of the orientation of molecular dipoles near charged surfaces. The present calculations were carried out for $\epsilon = 80$ and 30. The free energy functional must now include a term to account for the Coulombic interactions, in the form

$$F_{\mathrm{Coul}} = \frac{1}{2}\int_V \Psi(\mathbf{r})\rho_c(\mathbf{r})\, d\mathbf{r}\,, \qquad (6)$$

where $\rho_c(\mathbf{r})$ is the ionic charge density inside the channel and $\Psi(\mathbf{r})$ is the local electrostatic potential, related to $\rho_c(\mathbf{r})$ by Poisson's equation and satisfying appropriate boundary conditions on the surface of the channel. Even with this additional term, the variational problem (1) retains its one-dimensional (purely radial) character, so that numerical solutions of the resulting Euler-Lagrange equations are readily obtained. The electrostatic effects are illustrated in Fig. 4, where the relative absorbances ζ are plotted versus channel radius R for $\epsilon = \infty$ (equivalent to zero charge), $\epsilon = 80$ and 30. The general shape of the $\zeta(R)$ curves is independent of ϵ and quantitative differences are largely insignificant. However this "semiprimitive" model of the solvent cannot account for ion hydration and the gradual dehydration, for increasing confinement. In particular the model is intrinsically incapable of reproducing the dramatic change of ion density profiles observed in the simulations of Ref. [4] upon charging the ions in the presence of a realistic model for water.

The present DFT approach can, however, be refined to include a fully microscopic model of water, involving molecular values of the electric dipole and higher order multipole moments [14]. This will allow a self-consistent assessment of the relative importance of steric and electrostatic effects in determining the selectivity of cylindrical channels.

The model and DFT used here may also be generalized to more complicated pore topologies than the simple cylindrical shape considered so far. For instance, a somewhat more realistic representation of the KcsA channel [9] includes a spherical cavity, of radius $R_0 = 0.5$ nm, with two coaxial cylindrical segments on both sides (see Fig. 1). This topology still preserves cylindrical symmetry, but the translational invariance is lost, so that the density profiles $\rho_\alpha(\mathbf{r})$ now depend on two variables, r and z. We have solved the corresponding Euler-Lagrange equations on an (r, z) grid. Preliminary results for the model of a ternary mixture of neutral hard spheres point to a strong tendency of the smaller spheres (representing the Na^+ and K^+ ions) to be localized at the center of the spherical cavity while the larger (water) spheres tend to concentrate in the cylindrical end segments of the channel. Details of these results will be published elsewhere.

The authors thank Ruth Lynden-Bell for fruitful discussions. D. Goulding thanks the EPSRC for their support and S. Melchionna acknowledges the support of the Leverhulme Trust.

[1] S. Mohanty and A. W. McCormick, Chem. Eng. J. **74**, 1 (1999).
[2] B. Hille, *Ionic Channels in Excitable Membranes* (Sinauer, Sunderland, 1992), 2nd ed.; R. S. Eisenberg, Contemp. Phys. **39**, 447 (1998).
[3] B. Roux and M. Karplus, Annu. Rev. Biophys. Biomol. Struct. **23**, 731 (1994).
[4] R. M. Lynden-Bell and J. C. Rasaiah, J. Chem. Phys. **105**, 9266 (1996).
[5] M. S. Sansom, I. D. Kerr, J. Breed, and R. Sankararamakrishman, Biophys. J. **70**, 693 (1996).
[6] Q. Zhong, Q. Jiang, P. B. Moore, D. M. Newns, and M. L. Klein, Biophys. J. **74**, 3 (1998).
[7] T. W. Allen, S. Kuyucak, and S. H. Chung, Biophys. J. **77**, 2502 (1999).
[8] T. W. Allen, S. Kuyucak, and S. H. Chung, J. Chem. Phys. **111**, 7985 (1999).
[9] D. A. Doyle *et al.,* Science **280**, 69 (1998).
[10] J. L. Lebowitz and J. S. Rowlinson, J. Chem. Phys. **41**, 133 (1964).
[11] R. Evans, in *Fundamentals of Inhomogeneous Fluids,* edited by D. Henderson (Marcel Dekker, New York, 1992).
[12] Y. Rosenfeld, Phys. Rev. Lett. **63**, 980 (1989); Y. Rosenfeld, M. Schmidt, H. Löwen, and P. Tarazona, Phys. Rev. E. **55**, 4245 (1997).
[13] D. Frenkel and B. Smit, *Understanding Molecular Simulation* (Academic Press, London, 1996).
[14] P. G. Kusalik and G. N. Patey, J. Chem. Phys. **88**, 7715 (1988); M. Kinoshita, S. Iba, and M. Harada, J. Chem. Phys. **105**, 2487 (1996); T. Biben, J-P. Hansen, and Y. Rosenfeld, Phys. Rev. E **57**, R3727 (1998).